Eur. Phys. J. Appl. Phys. **54**, 10102 (2011)
DOI: 10.1051/epjap/2011100390

THE EUROPEAN PHYSICAL JOURNAL APPLIED PHYSICS

Regular Article

Extraction of equivalent circuit parameters of solar cell: influence of temperature

M. Khalis, Y. Mir, J. Hemine, and M. Zazoui[a]

Laboratory of Condensed Matter, Faculty of Sciences and Techniques, University of Hassan II Mohammedia, Casablanca, Avenue Hassan II, BP 146, 28800 Mohammedia, Morocco

Received: 5 October 2010 / Received in final form: 1st November 2010 / Accepted: 18 January 2011
Published online: 13 April 2011 –

Abstract. A new method to evaluate the five parameters of illuminated solar cells is described. The method is based on nonlinear least squares approach. On calculating the lsqcurvefit-function with constraints, between the experimental current-voltage $I(V)$ characteristic and a theoretical arbitrary characteristic based on Lambert W-function. The used model is implemented as a MATLAB® script which yields the $I(V)$ characteristics of the LILT under test. The model has been validated against by applying it to experimental $I(V)$ characteristics. Some parameters of the model have been measured directly whereas others have been evaluated by means of direct computation on the data sheet or by means of best-fit on the measured data. The results have been compared and an analysis of the errors is presented.

1 Introduction

The interest in using photovoltaic solar cells to power spacecraft for interplanetary missions began over almost five decades ago, fairly soon after the first Earth satellites were successfully launched. Initial choices included the nearby planets of Venus and Mars, although more ambitious efforts were also under evaluation. Early solar cell researchers quickly discovered a number of problems for solar cells operating at LILT [1–6] (low intensity low temperature) conditions. Obviously, operation at increasing solar distances reduces the available light suitable to the cell in accordance with the inverse square law [7] ($1/R^2$ – where R is the spacecraft distance to the Sun). As the solar intensity decreases, both photocurrent J_{SC} and T decrease. The actual cell temperature is related to the solar incidence, the array of absorptivity and emissivity, and thermal interactions with the spacecraft.

The knowledge of solar cell model parameters from measured current-voltage I-V characteristics is of vital importance for the quality control and evaluation of the performance of the solar cells. Several authors [8–26] proposed methods to devise ways for extracting the parameters that describe the non-linear electrical model of solar cells. These parameters are usually the saturation current, the series resistance, the ideality factor, the shunt resistance and the photocurrent. Some of the suggested methods involve both illuminated and dark I-V characteristics [27,28], while others use dynamic measurements [29,30] or integration procedures [31] based on the computation of the area under the current-voltage curves.

The approximation method, least-squares numerical techniques [32], is used to achieve the explicit solutions containing only common elementary functions. A careful search of the literature reveals that the use of a function known as Lambert W-function [33,34], commonly as "W-function", which is not frequently used in electronic problems is extremely important for solving such kind of problems. This W-function is defined by the solution of equation $W\exp(W) = x$: although rarely used, its properties are well documented [35–38] and several algorithms were published for calculating the W-function. Some recent work includes an exact analytical solution based on W-function for the case of a non-ideal diode model which comprises a single exponential and a series parasitic resistance. The current-voltage relation of solar cell is transcendental in nature; hence it is not possible to solve it for voltage in terms of current explicitly and vice versa.

This paper describes the use of W-function to find the explicit solution for the current and voltage and uses them to extract different parameters of solar cells. Comparisons are also made with the experimental data.

In this work we attempt to extract the five illuminated solar cell parameters. It is organized as follows: first, the theoretical background of the method used to extract the parameters is given. Then the results are discussed and compared with those in other works. Finally, we sum up with conclusions.

2 Theory and application

The single diode model assumes that the dark current can be described by a single exponential dependence modified

[a] e-mail: zazouimimoun@yahoo.fr

by the diode ideality factor n. The current-voltage relationship is given by:

$$I = I_{ph} - I_0 \left(\exp\left(\frac{V + IR_s}{nV_{th}} \right) - 1 \right) - \frac{V + IR_s}{R_{Sh}} \quad (1)$$

where I and V are terminal current and voltage in amperes and volts respectively, I_0 the junction reverse current (A), n the junction ideality factor and V_{th} the thermal voltage (KT/q), R_S and R_{Sh} are series and shunt resistance respectively, and I_{ph} the photocurrent. Equation (1) is transcendental in nature hence it is not possible to solve it for V in terms of I and vice versa. However, explicit solution for current and voltage can be expressed using W-function as follows:

$$I = -\frac{V}{R_S + R_{Sh}} - \frac{\text{LambertW}\left(\frac{R_S I_0 R_{Sh}}{nV_{th}(R_S+R_{Sh})} \exp\left(\frac{R_{Sh}\left(R_S I_{ph} + R_{Sh} I_0 + V\right)}{nV_{th}(R_S+R_{Sh})} \right) \right) nV_{th}}{R_S} + \left(\frac{R_S\,(I_0 + I_{ph})}{R_S + R_{Sh}} \right). \quad (2)$$

The concept of least squares is to fit a linear or nonlinear curve which fits that data best according to some criterion. One such common criterion is the minimization of the sum of the squared the differences between the actual data and the predicted data due to our least squares line. The error ε thus is defined as:

$$\varepsilon = \sum_{i=1}^{N} \left(I_i - I\left(V_i, p\right) \right)^2 \quad (3)$$

where N is the number of measured $I(V)$ pairs denoted by (V_i, I_i); $I(V, p)$ is the theoretical current for voltage V as predicted by a model containing several parameters represented by p that are the variables used to minimize the error.

This formulation amounts to minimize the difference between the measured points and the theoretical curve, and it is implicitly assumed that no measurement error affects the voltage data. But this is not generally true and the influence of experimental errors is misinterpreted [39].

To summarize, the proposed procedure consists of the following steps:

- data: N measures/observations $(V_i; I_i), i = 1, ..., N$;
- find: vector of k parameters (initial values) $p_0 = (p_{10}, ..., p_{k0})$, which gives the best fit has the function model $I(V, p)$, where I is a nonlinear function of p;
- define: function residual $r_i(p) = I_i - I(V_i, p), i = 1, ..., N$;
- minimize: to find the parameters p_k which minimize the error $\phi(p) = \frac{1}{2} r^T(p) r(p)$ i.e. vector gradient must be zero $\nabla\phi(p) = J^T(p) r(p) = 0$, necessary but not sufficient condition. J is the Jacobian of the $r(p)$: $J(P) = \frac{\partial(r_1, ... r_N)}{\partial(p_1, ... p_N)}$. Hessian matrix: $H(p) = \nabla^2\phi(p) = J^T(p)J(p) + \sum_{i=1}^{N} r_i(p) H_i(p)$, where $H_i(p)$ is the Hessian of $r(p_i)$.
  Method of Gauss-Newton:

$$\begin{cases} p_0 \\ H_k = \sum_{i=1}^{N} \nabla\Phi_i(p_k) \nabla\Phi_i(p_k)^{\perp}; \\ p_{k+1} = p_k - H_k^{-1} \nabla\Phi(p_k) \end{cases}$$

- display values of parameters: $I_{ph}; I_0; R_S; n; G_{Sh} = 1/R_{Sh}$ and the error ε;
- plotting: $I(V)$ curves.

This algorithm is implemented in the "lsqcurvefit" MATLAB® function.

In this work we will use the MATLAB® function "lsqcurvefit" which solves problems nonlinear least squares by minimizing the sum of the error function (ε) for extracting the cell parameters. We choose initial parameters to optimize this function. The function "lsqcurvefit" contains some other parameters for optimization. This feature offers the user to define domain boundaries definition of parameters. The first test was to limit the domain of definition of the parameters without a priori they are not affected. Thus to fit this function we have chosen the minimum and maximum limit: $Lb < P < Ub$ with $P = (I_{ph}, I_0, R_S, n, G_{Sh})$.

3 Results and discussion

To confirm our work, we will apply our approach to cell references [40–42]. We have tried to work on two cells, one is old, radio technique compelec (RTC) and the other is recent, light-pulsed solar simulator (LPSS) with a fill factor (FF) of 0.840 to reach a generalization. The results are given in Tables 1 and 2.

Using the method proposed here, for the solar cell references [40–42], the obtained results are compared with published data related to this device. The agreement between the obtained results and those published previously is remarkable. In Figures 1a and 1b below, the solid squares are the experimental data for the solar cell and the solid line is the fitted curve derived equation (1) with the parameters shown in Tables 1 and 2.

The Chegaar et al. [40] has fitted with four parameters using the conductance as a function. Using the derivation method to calculate $G_i = \frac{\partial I_i}{\partial V_i}$. He then deduced the I_{ph} with the relationship $I = f(V)$ at $V = 0$, this method induces experimental and theoretical errors.

In our method we have fitted five parameters at the same time, but although the Newton procedure converges rapidly, it has a major difficulty in converging to the solution; because the optimization is related to constraint and not free.

The illuminated $I(V)$ characteristics of LILT solar cells based on n^+pp^+ silicon grown by MOCVD are displayed in

Table 1. Optimal parameters obtained in references [40,41] and in this work at temperature 306 K.

P	In reference [41]	In reference [40]	Initial values	Constraints	Final values
G_{Sh} (Ω^{-1})	0.0186	0.0202	0.01	0–1	0.01515
R_S (Ω)	0.0364	0.0364	1	0–3	0.0447
n	1.4837	1.5039	1	0–3	1.3564
I_0 (μA)	0.3223	0.4039	1	0–10	0.10
I_{ph} (A)	0.7608	0.7609	0.1	0–1	0.7623

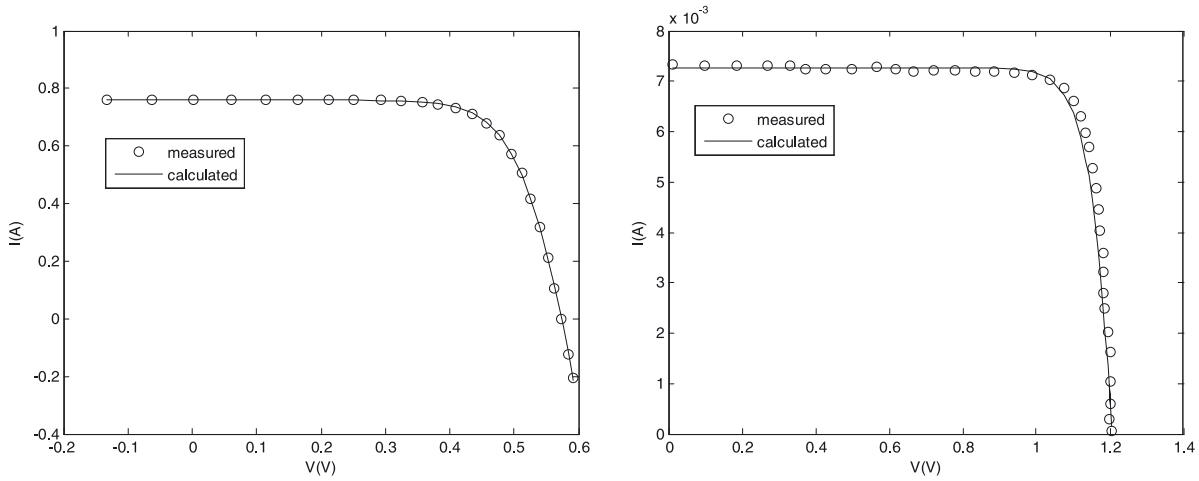

(a) (b)

Fig. 1. Experimental (∘) data and the fitted curve (–) for (a) the commercial (RTC) solar cell [40,41] and (b) LPSS, GaAs on GaAs, 0.25 cm^2 [42].

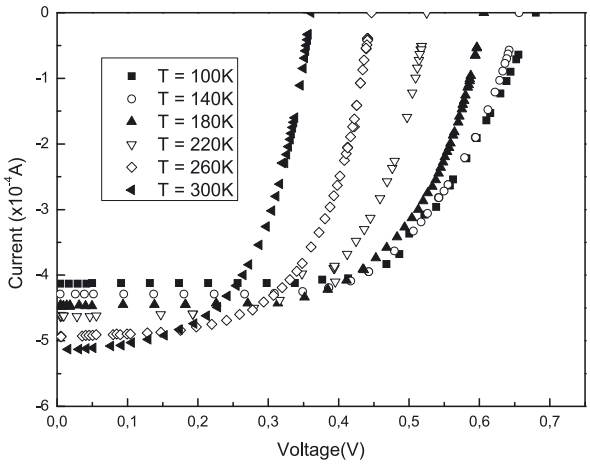

Fig. 2. I-V characteristic of solar cell in low intensity and low temperature conditions.

Figure 2 as measured under low intensity and low temperature conditions. The measurements have been performed in a vacuum chamber with quartz window, where the samples could be cooled by liquid nitrogen and the insolation intensity of the solar simulator has been done by xenon Lamp. These measures have been taken by an automated electronic device that was designed and developed by our research team.

The temperature of the solar cell in space is largely determined by the intensity and duration of its illumination, and also by its position relative to the sun. We have varied systematically the temperature from 100 K to 300 K to extract parameters of the cell.

In Figure 2 is presented the functional part of $I(V)$ characteristic at different temperature of the solar cell. It is bounded by the short circuit point ($V = 0, I = I_{sc}$) and open circuit point ($V = V_{OC}, I = 0$). Both points can be determined experimentally.

Figure 3 shows that when the temperature increases the open circuit voltage V_{OC} decreases linearly in the range from 140 to 300 K; below 140 K the variation of V_{OC} seems tends to saturate. Temperature coefficients are calculated by means of a least square method and we find $dV_{OC}/dT = -1.87$ mV K^{-1} for $T = 140$ to 300 K and $dI_{SC}/dT = 0.126$ μA K^{-1} (see Fig. 4) in good agreement with previous work [6].

In order to explain the photocurrent increase, when T increases from 100 to 300 K, we show in Figure 5 a spectral response of solar cell, for wavelengths varying from 350 nm to 1100 nm, when temperature varies from 120 K to 300 K. This figure shows that the spectral response varies in a weak manner. Then, the photocurrent increase can be explained by at least two different effects, a change in the contact metallization and a low internal shunt resistance. The results obtained show that the increase of the photocurrent is not due to reduction of the silicon energy band gap, but probably to parasitic resistance.

Figure 6 shows an I-V curve that result in a "flat" near the peak power point due to the metallization contact.

Table 2. Comparison between extracted values from [42] and extracted value using our method at temperature 298 K.

P	In reference [42]	Initial values	Constraints	Final values
G_{Sh} (Ω^{-1})	–	1.3×10^{-4}	0–10^{-2}	1.5×10^{-8}
R_S (Ω)	1.4	1.2	0–3	1.408
n	2	1.6	0–3	1.76
I_0 (A)	10^{-11}	10^{-14}	0–10^{-10}	2.24×10^{-14}
I_{ph} (A)	7.22×10^{-3}	2×10^{-4}	0–7.6×10^{-3}	7.26×10^{-3}

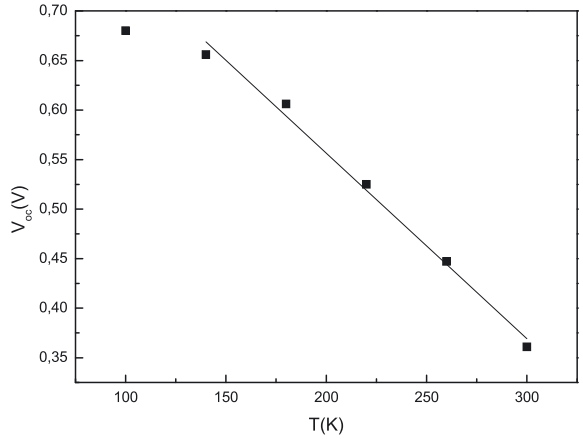

Fig. 3. Variations of the open-circuit voltage versus temperature.

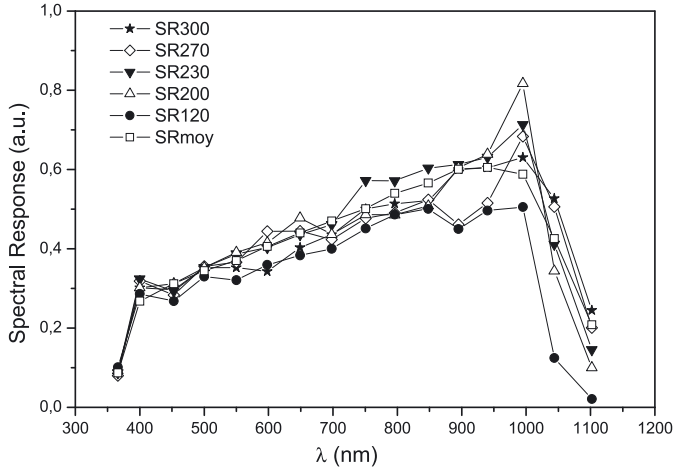

Fig. 5. Spectral response versus wavelengths for different temperature, the SRmoy is the average of the spectral response.

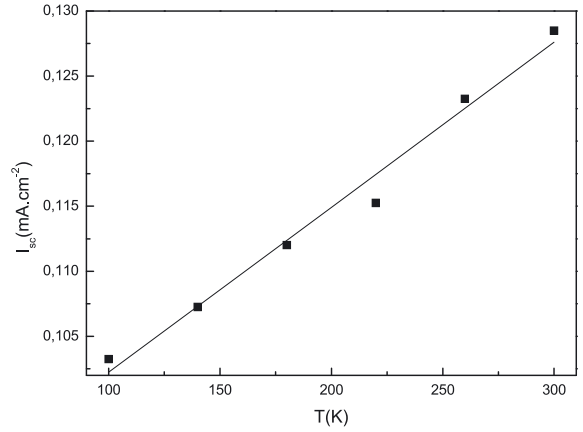

Fig. 4. Variations of the short-circuit current versus temperature.

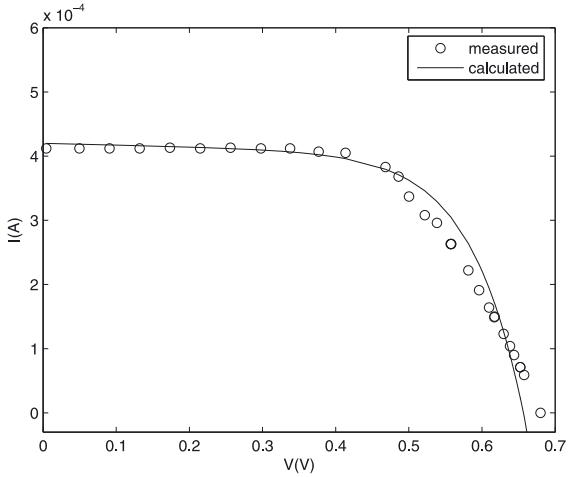

Fig. 6. Experimental (○) data and the fitted curve (–) for the LILT Si solar cell at 100 K.

In the region where the current should be constant, it is no longer as such, which explains the effect of shunt resistance.

Finally we apply our method to determine the five parameters for each temperature. The results are summarized in Table 3 and in Figures 6–8 some $I(V)$ characteristics of the cell in LILT condition for given temperatures with corresponding fitted curves are given. One notices that the fit did become increasingly better as the temperature increases. For low temperature, one noticeable default affecting the solar cells is the LILT effect. It is mainly due to two different defects.

The first one is a large internal series resistance. In fact, the large series resistance reduced the generated current. Therefore, the current flowing through the solar cell will be reduced as well as the voltage over the junction. The second defect is a diode in the contact metallization. These effects are responsible for diode currents loss and severe power losses with preference at low temperature. From Figures 6–8 we see that the fill factor has also increased from 57.24% at 300 K, to 67.10% at 180 K, rising to 76.75% at 100 K.

Table 3. Optimal parameters obtained in this work at different temperature.

P / T (K)	G_{Sh} (Ω^{-1})	R_S (Ω)	n	I_0 (μA)	I_{ph} (A)	ε
100	2.70×10^{-5}	8.40	8	3.10×10^{-8}	4.20×10^{-4}	4.91×10^{-8}
140	2.90×10^{-5}	5.3	5	1.10×10^{-8}	4.34×10^{-4}	5.65×10^{-8}
180	3.7×10^{-6}	4.86	4.6	1.10×10^{-7}	4.56×10^{-4}	1.2×10^{-8}
220	7.32×10^{-6}	3.76	3.54	2.23×10^{-7}	4.85×10^{-4}	1.438×10^{-8}
260	9.91×10^{-6}	2.80	2.67	3.16×10^{-7}	5.03×10^{-4}	8.166×10^{-9}
300	6.82×10^{-5}	2.40	2.26	1.15×10^{-6}	5.315×10^{-4}	7.04×10^{-9}

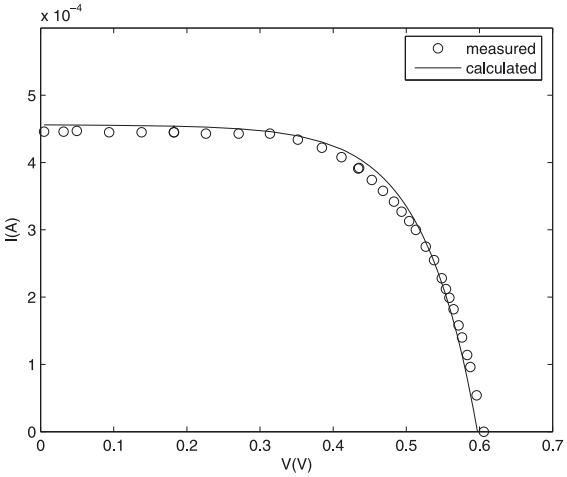

Fig. 7. Experimental (∘) data and the fitted curve (–) for the LILT Si solar cell at 180 K.

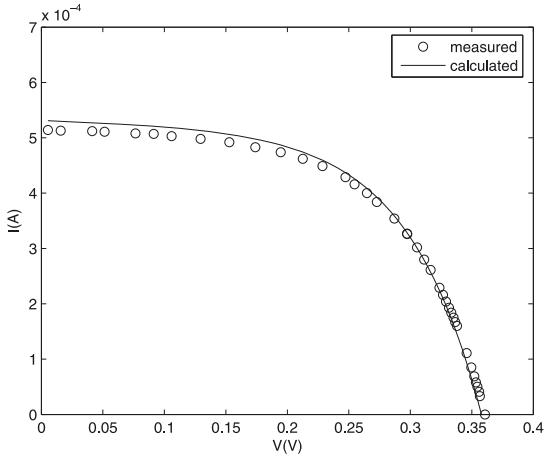

Fig. 8. Experimental (∘) data and the fitted curve (–) for the LILT Si solar cell at 300 K.

4 Conclusion

The paper presents a method to identify the parameters of the external characteristic $I(V)$ of a photovoltaic solar cell, considering as a starting point a model with five parameters. The method is based on using the nonlinear least squares algorithm; this algorithm is implemented in the "lsqcurvefit" MATLAB® function. The calculated results compares favourably with experimental data, thus validating the analysis. The sample solar cell LILT has been characterized at low intensity, low temperature conditions. A good fit of the experimental data is presented and the results are in good agreement with other works.

References

1. N.S. Fatemi, S. Sharma, O. Buitrago, J. Crisman, P.R. Sharps, R. Blok, M. Kroon, C. Jalink, R. Harris, P. Stella, S. Distefano, in *Conf. Record of the 31st IEEE Photovoltaic Specialists Conf., Lake Buena Vista, FL, USA, 2005*, p. 618
2. C.J. Gelderloos, K.B. Miller, R.J. Walters, G.P. Summers, S.R. Messenger, in *Conf. Record of the 39th IEEE Photovoltaic Specialists Conf., New Orleans, LA, USA, 2002*, p. 804
3. M. Imaizumi, R.D. Harris, R.J. Walters, J.R. Lorentzen, S.R. Messenger, J.G. Tischler, T. Ohshima, S. Sato, P.R. Sharps, N.S. Fatemi, *33rd IEEE Photovoltaic Specialists Conf. (PESC'08), Rhodes, Greece, 2008*
4. R. Campesato, C. Flores, IEEE Trans. Electron Dev. **38**, 6 (1991)
5. G. Strobl, P. Uebele, R. Kern, K. Roy, C. Flores, R. Campesato, C. Signorini, K. Bogus, in *1st WCPEC, Hawaii, HI, USA, 1994*, p. 2124
6. S. Brambillasca, F. Topputo, A. Finzi, R. Campesato, in *XX AIDAA Congress, Milano, Italy, 2009*, p. 3
7. P.M. Stella, F.S. Pool, M.A. Nicolet, P.A. Iles, Photovoltaic Energy Conversion, in *Conf. Record of the 24th IEEE Photovoltaic Specialists Conf., Waikoloa, HI, USA, 1994*, p. 199
8. D. Laplaze, I. Youm, Sol. Cells **14**, 167 (1985)
9. D. Laplaze, I. Youm, Sol. Cells **14**, 179 (1985)
10. A. Kaminski, J.J. Marchand, A. Laugier, *26th IEEE Photovoltaic Specialist Conf., Anaheim, CA, USA, 1997*
11. A. Kaminski, J.J. Marchand, A. Laugier, Solid State Electron. **43**, 741 (1999)
12. A.G. Aberle, S.R. Wenham, M.A. Green, in *23th IEEE Photovoltaic Specialist Conf., Louisville, KY, USA, 1993*, p. 133
13. E. Van Kerschaver, R. Einhaus, J. Szlufcik, J. Nijs, R. Merten, in *Proc. of 14th European Community Photovoltaic Solar Energy Conf., Barcelona, Spain, 1997*, p. 2438
14. P. Miahle, A. Khoury, J.P. Charle, Phys. Stat. Sol. A **83**, 403 (1984)
15. M. Bashahu, A. Habyarimana, Renew. Energy **6**, 129 (1995)

16. D.S.H. Chan, J.R. Phillps, J.C.H. Phang, Solid State Electron. **29**, 329 (1986)
17. P. Flavius-Maxim, T. Leonida-Dragomir, CEAI **12**, 30 (2010)
18. S. Dib, M. De la Bardonnie, A. Khoury, F. Pelanchon, P. Mialhe, Act. Passive Electron. Compon. **22**, 157 (1999)
19. K. Bouzidi, M. Cheggar, N. Nehou, *4th Int. Conf. on Computer Integrated Manifacturing CIP, Setif, Algeria, 2007*
20. A. Jain, A. Kapoo, Sol. Energy Mater. Sol. Cells **81**, 269 (2004)
21. M. Haouari-Merbah, M. Belhamel, I. Tobías, J.M. Ruiz, Sol. Energy Mater. Sol. Cells **87**, 225 (2005)
22. M. Bashahu, A. Habyarimana, Renew. Energy **6**, 129 (1995)
23. A. Malaoui, A. El Mansour, Revue Énergies Renouvelables **13**, 199 (2010)
24. A. Ortiz-Conde, J. Francisco García Sánchez, J. Muc, Sol. Energy Mater. Sol. Cells **90**, 352 (2006)
25. M. Chegaar, Z. Ouennoughi, F. Guechi, Vacuum **75**, 367 (2004)
26. M. Chegaar, G. Azzouzi, P. Mialhe, Solid State Electron. **50**, 1234 (2006)
27. M. Wolf, H. Rauschenbach, Adv. Energy Convers. **3**, 455 (1963)
28. M.S. Imamura, J.I. Portschheller, in *Proc. of 8th IEEE Photovoltaic Specialist Conf., Seattle, WA, USA, 1970*, p. 102
29. J.P. Charles, M. Abdelkrim, Y.H. Muoy, P. Mialhe, Sol. Cells **4**, 169 (1981)
30. S.K. Agrawal, R. Muralidharam, A. Agrawala, V.K. Tewary, S.C. Jain, J. Phys. **14**, 1634 (1981)
31. G.L. Araujo, E. Sanchez, IEEE Trans. Electron Dev. **29**, 1511 (1982)
32. S.K. Datta, Solid State Electron. **35**, 1667 (1992)
33. T.C. Banwell, A. Jayakumar, Electron. Lett. **36**, 291 (2000)
34. A. Oritz-Conde, F.J. Garcia, Solid State Electron. **440**, 186 (2000)
35. D.A. Barry, P.J. Culligan-Hensley, S.J. Barry, ACM Trans. Math. Software **21**, 161 (1995)
36. D.A. Barry, P.J.C. Hensley, S.J. Barry, ACM Trans. Math. Software **21**, 172 (1995)
37. R.M. Corless, G.H. Gonnet, D.E.G. Hare, D.J. Jeffry, D.E. Kunth, ACM Trans. Math. Software **5**, 329 (1996)
38. F.N. Fritsch, R.E. Shafer, W.P. Crowley, Commun. ACM **16**, 123 (1973)
39. V. Martínez, R. Lizundia, J.C. Jimeno, in *Proc. of 11th EC PVSEC, Montreux, Switzerland, 2003*, p. 314
40. M. Chegaar, Z. Ouennoughi, A. Hoffmann, Solid State Electron. **45**, 293 (2001)
41. T. Easwarakhanthan, J. Bottin, I. Bouhouch, C. Boutrit, Int. J. Sol. Energy **4**, 1 (1986)
42. K. Takahashi, S. Yamada, T. Unno, S. Kuma, Sol. Energy Mater. Sol. Cells **50**, 169 (1998)